



Asian Journal of Scientific Research

ISSN 1992-1454

science
alert
<http://www.scialert.net>

ANSI*net*
an open access publisher
<http://ansinet.com>

One-pot Synthesis of Oil Dispersible Ultra Fine Manganese (II) Oxide Nanoparticles

Naresh Yandrapalli and K.S. Rajan

Centre for Nanotechnology and Advanced Biomaterials (CeNTAB), School of Chemical and Biotechnology, SASTRA University, Thanjavur 613 401, India

Corresponding Author: K.S. Rajan, Seshasayee Paper and Boards Chair Professor in Chemical Engineering, Centre for Nanotechnology and Advanced Biomaterials (CeNTAB), School of Chemical and Biotechnology, SASTRA University, Thanjavur-613401, India Tel: +919790377951 Fax: +91-4362-264120

ABSTRACT

Nanoparticles have attracted lot of attention for their exceptional properties which are different from those of materials in bulks. Metal oxides have shown application in many domains of science. Especially, manganese oxide has proven applications in energy storage, sensors, imaging technologies and even biomedicine. But, synthesis of ultrafine monodisperse nanoparticles that can be dispersed easily in polar or non-polar solvent is of prime importance for applications involving composites, phase change energy material, thermal management etc. We report the synthesis of ultrafine monodisperse MnO nanoparticles from manganese acetate tetrahydrate by a solvothermal method. Surfactants, oleic acid and 1-octadecene were used in suitable concentrations to yield oleic acid stabilized manganese oxide nanoparticles. The formation of manganese-oleate complex in the first step was confirmed using FTIR. X-ray diffraction spectra confirmed the formation of manganese oxide. Scanning and Transmission Electron Micrographs established the size of nanoparticles to be in the range of 15-20 nm. Crystalline nature of the nanoparticles was confirmed using selected area electron diffraction. Aging time has been found to influence the size of the nanoparticles, with larger particle sizes obtained for higher aging periods. These nanoparticles are suitable for dispersion in non-polar solvents and in thermic fluids like Therminol® 55 resulting in nanofluids.

Key words: Manganese oxide, nanoparticles, monodisperse, oleic acid, Therminol-55®

INTRODUCTION

Magnetic nanoparticles are of great interest to researchers and scientists for their potential applications in wide variety of disciplines including catalysis, biomedicine, sensors, imaging, data storage and environmental remediation (Natalie *et al.*, 2009; Bae *et al.*, 2011; Sljukic *et al.*, 2011; Lu *et al.*, 2004; Elliott and Zhang, 2001).

There are several materials that exhibit magnetic properties (Roca *et al.*, 2009). Especially, metal oxides like iron oxide, cobalt oxide have multiple applications (Roca *et al.*, 2009). Despite the identification of several magnetic materials, there is a necessity for the advent of new magnetic nanoparticles which can be used in multiple domains of science. One such prospective metal oxide is manganese oxide. Currently, manganese oxide is known for its catalytic properties and energy storing capabilities (Lee *et al.*, 2005). Manganese oxides are structurally versatile capable of being existent in the form of around 15 allotropes and possess numerous attainable oxidation states

(Portehault *et al.*, 2009). This imparts dimensionality specific effects on electronic, electrochemical and magnetic properties (Subramanian *et al.*, 2008). The impact of structure on electrochemical behavior of manganese oxide nanoparticles has been reported (Lee *et al.*, 2005). Manganese oxide nanoparticles by virtue of their high surface area and superparamagnetic nature under certain circumstances are interesting functional materials. Manganese oxide nanoparticles are gaining importance as MR contrast agents due to their capability to achieve T_1 -relaxation similar to that of gadolinium (Shin *et al.*, 2009; Gilad *et al.*, 2008). Surface area is important for applications involving fluid-particle heat transfer in all geometries (Rajan *et al.*, 2006-2008).

To harness the properties of manganese (II) oxide (MnO) nanoparticles for different applications, it is essential to synthesize monodisperse MnO nanoparticles. Here, we report our attempts to synthesize highly monodisperse manganese oxide nanoparticles using manganese acetate tetrahydrate as a precursor. The effect of aging time on the size of the nanoparticles obtained is also reported. Stable dispersions of MnO in Therminol-55[®] have been prepared using these nanoparticles.

MATERIALS AND METHODS

Materials: Manganese acetate tetrahydrate ($\geq 99\%$, Sigma Aldrich, India), Oleic acid (88%, Merck, India), 1-Octadecene (90%, Sigma Aldrich, India), n-Hexane (99%, Merck, India) and Acetone (99.9%, Merck, India) were procured used without any further purification. Therminol-55[®], a synthetic heat transfer fluid comprising hydrocarbon mixtures was procured from Solutia, USA.

Methods

Synthesis of MnO nanoparticles: The 1.386 g of manganese (II) acetate tetra hydrate was added to a round bottomed flask containing 6.981 g oleic acid. The flask was heated to 180°C in a heating mantle. After this temperature was reached, the contents were left undisturbed for 2 h to enable the formation of metal-oleate complex. Later 23.67 g of 1-octadecene was added to the liquefied mixture and was heated to 310°C at a heating rate of 4°C min⁻¹ and allowed to age at that temperature for about 45 min. The solution was cooled to room temperature and precipitated using hexane and acetone. Excess and unreacted surfactants and ligands were removed from the precipitate by multiple washes with hexane and acetone followed by centrifugation. A waxy precipitate was obtained which was further analyzed for the presence of MnO nanoparticles. To study the effect of reaction time on the size of nanoparticles, the above procedure was repeated with different aging times of 1 and 2 h.

Preparation of MnO dispersions in Therminol-55[®]: A predetermined mass of MnO nanoparticles was added to 50 mL of Therminol-55[®] and dispersed using a high-shear homogenizer (IKA[®]T-25, Ultra Turrax, Germany).

CHARACTERIZATION OF NANOPARTICLES AND THE DISPERSION

Fourier transform infrared spectroscopy: The vibrational spectra of the precursor, intermediate and the product were recorded using a FTIR spectrometer (Spectrum100, Perkin Elmer, USA). The spectra were recorded in the wave number range of 400 to 4000 cm⁻¹, with an interval of 4 cm⁻¹, by averaging the four scans obtained for each sample.

X-ray diffraction studies: To ascertain the crystalline nature and phases of the synthesized material, X-ray diffractograms were recorded using a X-ray Diffractometer (X'PERT PRO MPD, PANalytical, Netherlands). Diffraction pattern were recorded for '2 θ ' in the range of 10 to 80° in steps of 0.05° at a scan rate of 0.1 steps per second.

Scanning electron microscopy: The surface morphology of the particles was observed using a Field Emission Scanning Electron Microscope (JSM 6701F, JEOL, Japan). Samples for microscopy were prepared by mounting powder on a brass stub using double sided carbon tape. A thin layer of platinum was sputtered at a current of 20 mA for 45 sec to form a conducting layer. The sputter coated samples were then introduced into the specimen chamber of the electron microscope through the exchange chamber. An accelerating voltage of 3 kV was used to image the samples at ultra-high vacuum using the secondary electron detector.

Transmission electron microscopy: Transmission electron micrographs were obtained using a 200 kV, Field Emission Transmission Electron Microscope (JEM 2100F, JEOL, Japan). Nanoparticles were dispersed in n-hexane and a drop of this dispersion was used directly on the copper grid. Selected Area Electron Diffraction (SAED) pattern was also observed to ascertain the lattice parameters.

Dynamic light scattering: The particle size distribution of the dispersions was determined by Dynamic Light Scattering Technique using a Zetasizer (Nano-ZS, MALVERN Instruments, USA) at room temperature. The dispersions were suitably diluted to record the size distribution.

RESULTS

Figure 1 shows the FT-IR spectra of manganese acetate tetrahydrate (precursor), product from the first step and the final product. Bands at 2922, 2852, 1576 and 1431 cm^{-1} , respectively are

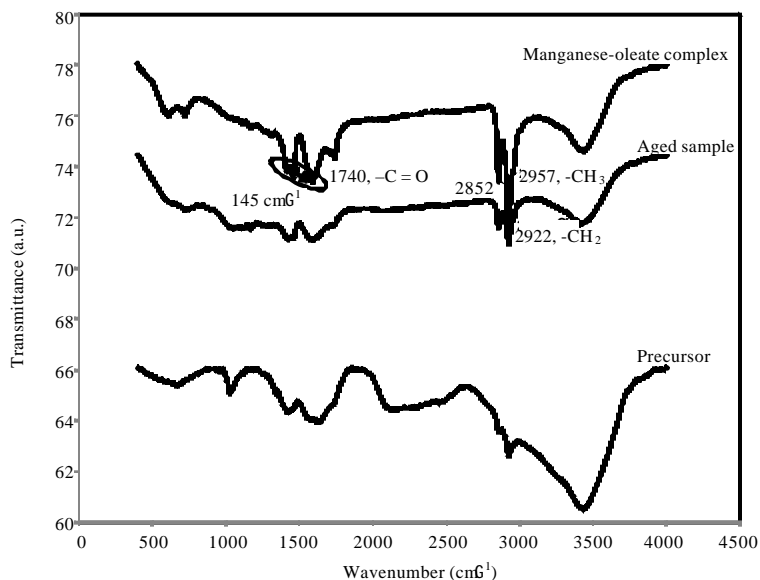


Fig. 1: FT-IR spectra of the manganese-oleate complex, aged sample and precursor (manganese (II) acetate tetrahydrate)

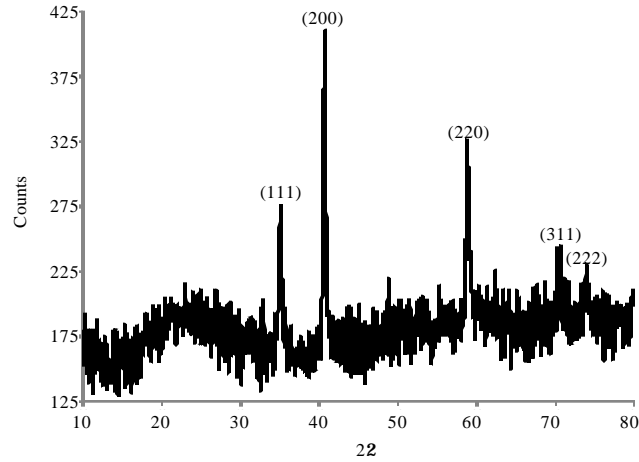


Fig. 2: X-ray diffractogram of MnO nanoparticles

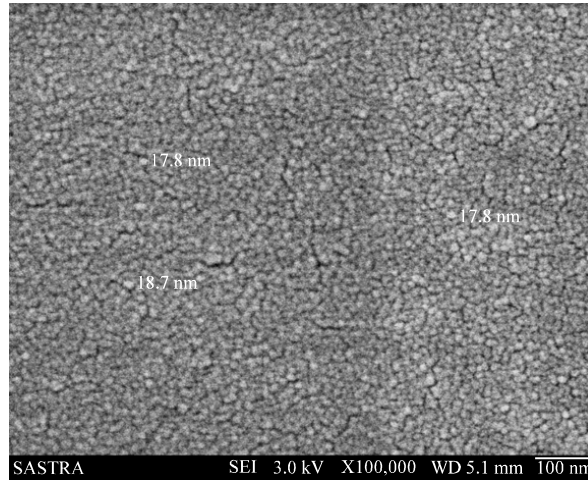


Fig. 3: Scanning electron micrograph of synthesized nanoparticles, showing high monodispersity in size and shape

visible for metal-oleate complex. Absorption for Mn-O stretching observed for metal-oleate complex disappears for the aged sample.

Figure 2 shows the X-ray diffraction of the synthesized nanoparticles. The average size of the particle is estimated using Scherrer equation which is as follows:

$$D = \frac{k\lambda}{\beta_{hkl} \cos\theta_{hkl}}$$

where, D is the crystallite size, k is constant (0.9), β_{hkl} is the full width at half maximum of the diffraction peak, θ_{hkl} is the Bragg's angle of the peak, λ is the wavelength of the X-ray (0.154 nm). Using the Scherrer equation, the average crystallite size was found to be 19 nm.

Figure 3 shows the scanning electron micrograph of MnO powders synthesized with an aging time of 45 min. It may be observed from Fig. 3 that nearly monodisperse MnO nanoparticles in

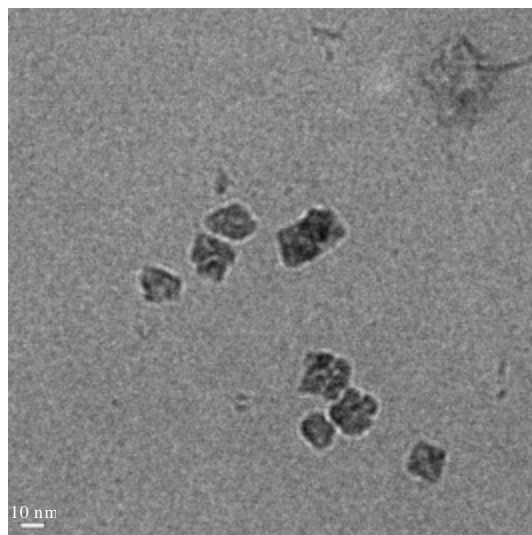


Fig. 4: Transmission electron micrograph of the manganese oxide nanoparticles

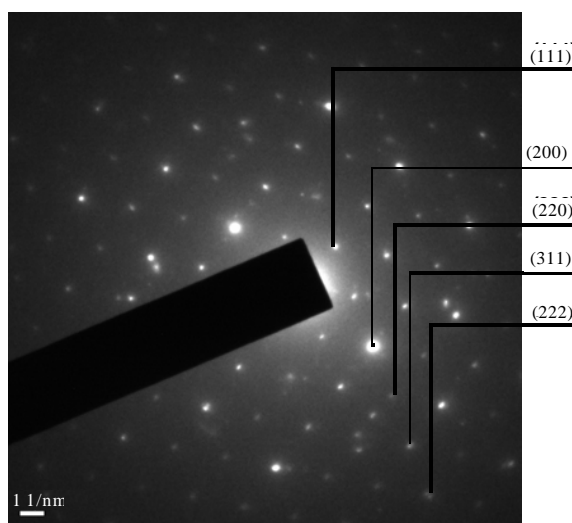


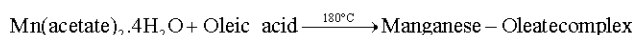
Fig. 5: Selected area electron diffraction (SAED) of manganese oxide nanoparticles

the size range of 15-20 nm were obtained. The high homogeneity with respect to particle shape and size are also evident from transmission electron micrographs (Fig. 4). Crystalline nature of the nanoparticles was confirmed by selected area electron diffraction which showed that the particles obtained were of highly crystalline in nature (Fig. 5).

DISCUSSION

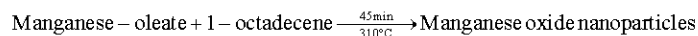
Reactions: The synthesis of MnO nanoparticles using $\text{Mn}(\text{acetate})_2$ and MnCl_2 as precursors has been reported (Kim *et al.*, 2011; Park *et al.*, 2004). The procedure adopted here is different from the

majority of those reported in the literature, as far as the second part of the synthesis is concerned, which is similar to that adopted by Thomas *et al.* (2009), who had followed a different procedure for the first step. In nut shell, our procedure has been designed by carefully studying the various existing protocols and making appropriate modifications. Also, in the first part of the synthesis, oleic acid has been used in excess in the present work, to ensure the complete conversion of precursor to manganese-oleate by the following reaction:



Higher temperature may enhance the rate of conversion of manganese acetate to manganese-oleate. However the decomposition temperature of the manganese-oleate complex is close to 220°C (Thomas *et al.*, 2009). Hence, taking above factors into consideration, a temperature of 180°C was chosen for the above reaction. Oleic acid is proven to have good ligation properties, stabilizing properties and also environmental friendly.

During the second step which involves heating the manganese-oleate and excess oleic acid in 1-Octadecene, nucleation of MnO is expected to begin at 220°C, the temperature for the onset of breakage of manganese-oleate, as per the following reaction:



It has been reported that the separation of nucleation and growth stages that occur at different temperatures would result in the formation of monodisperse metal oxide nanoparticles (Park *et al.*, 2004; Thomas *et al.*, 2009). Aging at the nucleation temperature would result in the formation of polydisperse amorphous product (Park *et al.*, 2004). Hence the growth was carried out at 310°C, close to the boiling point of 1-octadecene.

The formation of metal-oleate complex after the first step of the reaction was confirmed through FT-IR spectra, shown in Fig. 1. The FT-IR spectra show the presence of characteristic bands of the oleyl group such as the symmetric and asymmetric -CH₂ stretching at 2922 and 2852 cm⁻¹, respectively (Thomas *et al.*, 2009). Furthermore, the difference of 145 cm⁻¹ between strong absorption bands assigned to the asymmetric and symmetric stretching bands of the RCOO-group appear at 1576 and 1431 cm⁻¹, respectively, is characteristic for a bidentate coordination of the carboxylate to a metal atom (Thomas *et al.*, 2009; Alcock *et al.*, 1976; Barman and Vasudevan, 2007). Moreover, these characteristic bands of the oleyl group were absent in the precursor spectra. Hence from the FTIR spectra and the above discussion, the formation of metal-oleate complex is confirmed.

A careful investigation of FT-IR spectra of the aged sample shows relatively low intense peaks. Moreover, absorption for Mn-O stretching observed for manganese oleate complex disappeared for the aged sample. The Presence of -OH peak in metal-oleate complex may be due to the excess oleic acid used. There are reports of manganese binding to only two ligands (Thomas *et al.*, 2009) which invariably leave unreacted oleic acid.

The peaks observed in X-ray diffractograms (Fig. 2) correspond to the various crystal planes (111), (200), (220), (311), (222) of MnO (Yin and O'Brien, 2003).

Effect of aging time on morphology: It may be recalled that the nucleation of the MnO particles during the initial step at 240°C while their growth takes place at higher temperatures. The growth kinetics is predominantly influenced by temperature. With increased aging time at the

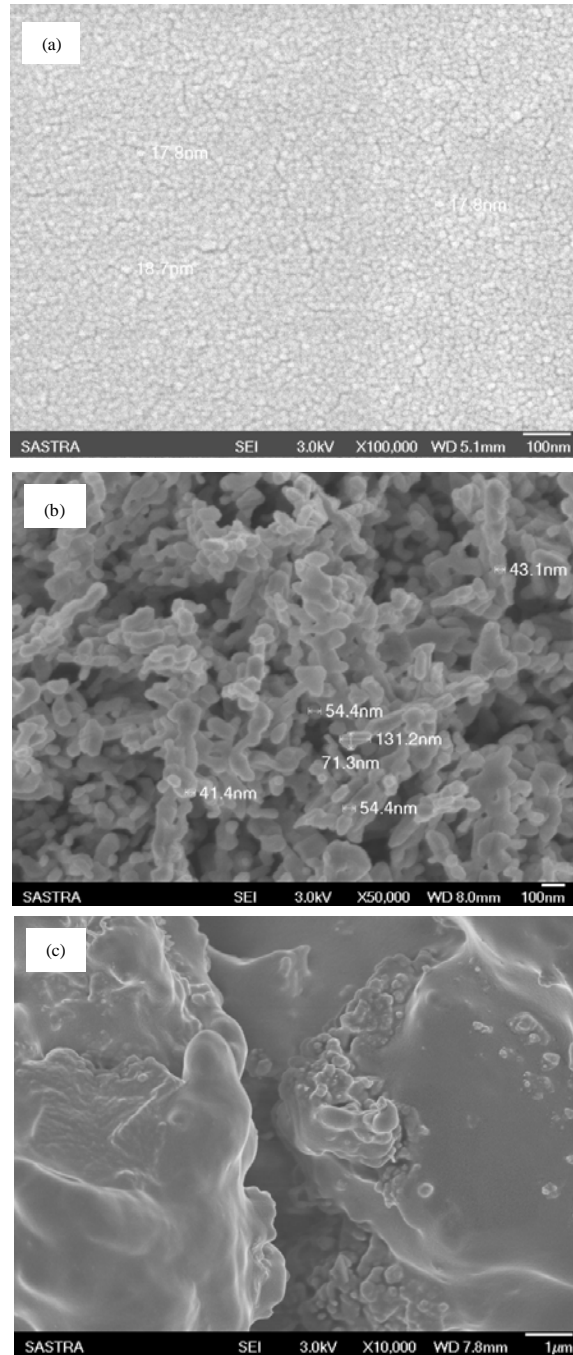


Fig. 6(a-c): Effect of aging time on the size of nanoparticles; (a) 45 min, (b) 1 h and (c) 2 h

growth temperature, crystals are expected to grow more resulting in their increased size. When the crystals grow such that they are in proximity to adjacent crystal, coalescence may occur as evident in FE-SEM micrographs in Fig. 6 for 1 h aging. With further increased aging time the particles might coalesce to form sheet like structures (Fig. 6) where the individual particles are difficult to

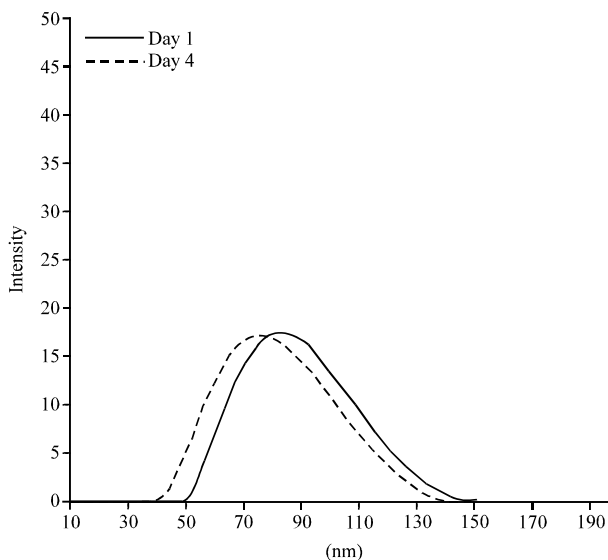


Fig. 7: Dynamic light scattering recording of MnO-Therminol-55[®] dispersions during day 1 and day 4

identify. Hence, the choice of optimum aging time is crucial for the synthesis of controlled, mono-disperse MnO nanoparticles.

Dispersion in Therminol-55: The dispersion of metal oxide in hydrocarbon liquids is a challenging task. Oleic acid is a popular dispersant for preparing dispersions of nanoparticles in oils. During the aging step, excess oleic acid could be adsorbed on the surface of the MnO nanoparticles, with the hydrocarbon chain pointing outward, enabling dispersion in hydrocarbon liquids. Hence, the MnO nanoparticles dispersed in Therminol-55[®] exhibited high colloidal stability for a long period of time. The particle size distribution measured over a period of four days showed (Fig. 7) negligible change in distribution which could be ascertained to the high colloidal stability caused by steric repulsion.

CONCLUSION

Although synthesis of monodisperse nanoparticles is a challenge, advances in the synthesis methods have made it possible. Especially, organic method of synthesizing nanoparticles is yielding nanoparticles with high uniformity in size, shape and crystalline. Our results once again proved the solidarity of this method. Highly crystalline nanoparticles with uniformity in size have been proposed. Oleic acid as a surfactant is highly stable and environment friendly can be of great use as ligand. 1-Octadecene is a perfect high boiling solvent for nanoparticles synthesis, when used around 280 to 320°C. Manganese (II) oxide nanoparticles have many applications in the near future by virtue of its magnetic properties and catalytic properties. Our results demonstrate that the MnO nanoparticles synthesized by the reported procedure can be dispersed easily in hydrocarbon liquids.

ACKNOWLEDGMENTS

This study is supported by (i) PG teaching grant No: SR/NM/PG-16/2007 of Nano Mission Council, Department of Science and Technology (DST), India (ii) Grant No: SR/FT/ET-061/2008, DST, India and (iii) Research and Modernization Project No. 1, SASTRA University, India.

REFERENCES

- Alcock, N.W., V.M. Tracy and T.C. Waddington, 1976. Acetates and acetato-complexes. Part 2. Spectroscopic studies. *J. Chem. Soc., Dalton Trans.*, 1976: 2243-2246.
- Bae, K.H., K. Lee, C. Kim and T.G. Park, 2011. Surface functionalized hollow manganese oxide nanoparticles for cancer targeted siRNA delivery and magnetic resonance imaging. *Biomaterials*, 32: 176-184.
- Barman, S. and S. Vasudevan, 2007. Mixed saturated-unsaturated fatty-acid salt assemblies: Solid solutions of zinc stearate and oleate. *J. Phys. Chem. B*, 111: 5212-5217.
- Elliott, D. W. and W.X. Zhang, 2001. Field assessment of nanoscale bimetallic particles for groundwater treatment. *Environ. Sci. Technol.*, 35: 4922-4926.
- Gilad, A.A., P. Walczak, M.T. McMahon, Hyon Bin Na and J.H. Lee *et al.*, 2008. MR tracking of transplanted cells with positive contrast using manganese oxide nanoparticles. *Magn. Reson. Med.*, 60: 1-7.
- Kim, T., M. Eric, J. Choi, K. Yuan and H. Zaidi *et al.*, 2011. Mesoporous silica-coated hollow manganese oxide nanoparticles as positive T1 contrast agents for labeling and MRI tracking of adipose-derived mesenchymal stem cells. *J. Am. Chem. Soc.*, 113: 2955-2961.
- Lee, C.Y., H.M. Tsai, H.J. Chuang, S.Y. Li, P. Lin and T.Y. Tseng, 2005. Characteristics and electrochemical performance of supercapacitors with manganese Oxide-carbon nanotube nanocomposite electrodes. *J. Electrochem. Soc.*, 152: A716-A720.
- Lu, A.H., W. Schmidt, N. Matoussevitch, H. Bonnermann and B. Spliethoff *et al.*, 2004. Nanoengineering of a magnetically separable hydrogenation catalyst. *Angew. Chem.*, 43: 4303-4306.
- Natalie, A.F., S. Peng, K. Cheng and S. Sun, 2009. Magnetic nanoparticles: Synthesis, functionalization and applications in bioimaging and magnetic energy storage. *Chem. Soc. Rev.*, 38: 2532-2542.
- Park, J., K. Hwang, Y. Park, J.G. Noh and H. Jin, 2004. Ultra-large-scale syntheses of monodisperse nanocrystals. *Nature Materials*, 3: 891-895.
- Portehault, D., S. Cassaignon, E. Baudrin and J.P. Jolivet, 2009. Structural and morphological control of manganese oxide nanoparticles upon soft aqueous precipitation through $\text{MnO}_4^-/\text{Mn}^{2+}$ reaction. *J. Mater. Chem.*, 19: 2407-2416.
- Rajan, K.S., S.N. Srivastava, B. Pitchumani and B. Mohanty, 2006. Simulation of gas-solid heat transfer during pneumatic conveying: Use of multiple gas inlets along the duct. *Int. Commun. Heat Mass*, 33: 1234-1242.
- Rajan, K.S., S.N. Srivastava, B. Pitchumani and B. Mohanty, 2007. Simulation of countercurrent gas-solid heat exchanger: Effect of solid loading ratio and particle size. *Appl. Therm. Eng.*, 27: 1345-1351.
- Rajan, K.S., K. Dhasandhan, S.N. Srivastava and B. Pitchumani, 2008. Studies on gas-solid heat transfer during pneumatic conveying. *Int. J. Heat Mass Trans.*, 51: 2801-2813.
- Roca, A.G., R. Costo, A.F. Rebolledo, S. Veintemillas-Verdaguer and P. Tartaj *et al.*, 2009. Progress in the preparation of magnetic nanoparticles for applications in biomedicine. *J. Phys. D: Appl. Phys.*, Vol. 42, 10.1088/0022-3727/42/22/224002.
- Shin, J., R.M. Anisur, M.K. Ko, G.H. Im, J.H. Lee and I.S. Lee, 2009. Hollow manganese oxide nanoparticles as multifunctional agents for magnetic resonance imaging and drug delivery. *Angew. Chem. Int. Ed.*, 48: 321-324.

- Sljukic, B.R., R.O. Kadara and C.E. Banks, 2011. Disposable manganese oxide screen printed electrodes for electroanalytical sensing. *Anal. Methods*, 3: 105-109.
- Subramanian, V., H. Zhu and B. Wei, 2008. Nanostructured manganese oxides and their composites with carbon nanotubes as electrode materials for energy storage devices. *Pure Appl. Chem.*, 80: 2327-2343.
- Thomas, D.S., T. Graf and W. Tremel, 2009. Synthesis and characterization of monodisperse manganese oxide Nanoparticles -evaluation of the nucleation and growth mechanism. *Chem. Mater*, 21: 3183-3190.
- Yin, M. and S. O'Brien, 2003. Synthesis of monodisperse nanocrystals of manganese oxides. *J. Am. Chem. Soc.*, 125: 10180-10181.